minerals

MDPI

Article

Distribution Characteristics of Trace Elements in Carboniferous–Permian Coal from the Western Margin of Ordos Basin: Emphasis on Their Complex Geological Genesis

Yaofeng Sun [1], Shaohu Li [1], Xin Dong [1], Wenjing Chen [1], Wei Song [1], Yinuo Zhang [1], Kexin Sun [1] and Guohong Qin [2,*]

[1] Institute of Environmental Geology, Hebei Coal Geology Bureau, Shijiazhuang 050024, China; 15076129081@163.com (Y.S.); shaoli079@126.com (S.L.); dongx796@126.com (X.D.); wen97899@yeah.net (W.C.); ws5673@sina.cn (W.S.); yinz234@yeah.net (Y.Z.); pb7612@outlook.com (K.S.)

[2] School of Geographical Sciences, Hebei Key Laboratory of Environmental Change and Ecological Construction, Hebei Normal University, Shijiazhuang 050024, China

* Correspondence: qinguohong1@163.com

Abstract: The Carboniferous–Permian coal deposits in the western margin of the Ordos Basin are known for their unique geological characteristics and potential enrichment of trace elements; however, there have been limited studies on the complex geological genesis of these elements, hindering the development of effective strategies for mineral resource exploration in this region. This study aims to investigate the distribution characteristics of trace elements in Carboniferous–Permian coal from the western margin of Ordos Basin, focusing on their complex geological genesis using techniques such as optical microscopy, X-ray fluorescence spectrometry, and inductively coupled plasma mass spectrometry. The results show that the average maximum vitrinite reflectance values in the Helanshan coalfield, Zhuozishan coalfield, and Ningdong coalfield are 1.25%, 0.83%, and 0.69%, respectively. Compared with the world's hard coals, Li and Ga in Carboniferous–Permian coal from the western margin of the Ordos Basin are mildly enriched (CC, concentration coefficients; $2 < CC < 5$) or enriched ($5 < CC < 10$). On the basis of revealing the response of the geochemical characteristics of coal to the geological development of the basin, the composite genetic model of terrigenous clastic supply, fault structure, low-temperature hydrothermal fluid and coal metamorphism have been established in Carboniferous–Permian coal in the western margin of the Ordos Basin. In this complex genetic model, folds and faults are very well developed. Although the provenance may have provided sufficient detrital sources for the study area, frequent tectonic changes, denudation, or scour led to the loss of detrital supply, and the provenance did not ultimately cause the enrichment of elements in the study area. However, the widely developed fault structure provided channels for sulfur-containing hydrothermal fluids, and the increase in coal metamorphism resulted in the enrichment of trace elements in the Carboniferous–Permian coal in the western margin of the Ordos Basin.

Keywords: western margin of Ordos Basin; Carboniferous–Permian coal; trace elements; geological genesis

Citation: Sun, Y.; Li, S.; Dong, X.; Chen, W.; Song, W.; Zhang, Y.; Sun, K.; Qin, G. Distribution Characteristics of Trace Elements in Carboniferous–Permian Coal from the Western Margin of Ordos Basin: Emphasis on Their Complex Geological Genesis. *Minerals* **2024**, *14*, 1136. https://doi.org/10.3390/min14111136

Academic Editor: Thomas Gentzis

Received: 3 October 2024
Revised: 29 October 2024
Accepted: 8 November 2024
Published: 10 November 2024

1. Introduction

In the process of the green transformation and sustainable utilization of coal resources, it is crucial to pay attention to the distribution, migration, and origin of trace elements in coal. The main material composition of coal is organic matter, which determines that the composition of coal has adsorption and reduction properties. Coal accumulates many kinds of trace elements under specific geological and geochemical conditions that reach the available degree and scale [1–4]. The enrichment of trace elements in coal is a complex process influenced by multiple factors. The primary factors identified in the Ordos Basin include provenance [5–10], sedimentary environment [11–14], volcanic ash [15,16],

groundwater activity [6,17], and coal metamorphism [18]. Provenance plays a crucial role in determining the initial elemental composition of the peat, which eventually forms coal [5]. The depositional environment, including pH value, redox, and ion concentration, are crucial factors influencing the enrichment of trace elements in coal [14]. The volcanic ash is rich in rare metal elements, which can be captured and enriched by coal seams during the deposition process of volcanic ash [16]. Groundwater activity can mobilize and redistribute trace elements within the coal seam [6]. Coal metamorphism refers to the changes in the physical and chemical properties of coal during burial and heating. These changes are primarily driven by temperature and pressure increases as the coal is buried deeper. Metamorphism affects the structure, composition, and reactivity of coal, including its trace element content. As coal undergoes metamorphism, its maceral composition changes, and trace elements may be redistributed or concentrated within specific mineral phases [18]. Recently, researchers have studied the occurrence and enrichment characteristics of trace elements in coal in the Ordos Basin. Dai et al. investigated the mineralogy and geochemical properties of the Junger coalfield, discovering an abnormal enrichment of boehmite and its unique mineral composition in the No. 6 super thick coal seam [5,6]. Sun et al. have thoroughly explored the genetic mechanism behind the exceptionally enriched Al-Li-Ga-REY polymetallic deposit found in the coal of the Junger coalfield [19]. Li et al. discovered that in the Buertaohai-Tianjiashiban mining area of the Junger coalfield, lithium is primarily found in silicoaluminate minerals, while gallium and fluorine are primarily linked to boehmite and organic matter [20]. Qin et al. analyzed the source of trace element enrichment in northeastern Ordos Basin coal, revealing that the peat formation environment influences the accumulation of Ga, Li, and REY elements in coal [21].

The western margin of the Ordos Basin occupies a unique structural position where the Alxa block, Qilian tectonic zone, Yinshan tectonic zone, Qinling tectonic zone, and Ordos block converge. Due to the special structural location, the tectonic environment, sedimentary formation development and trace element enrichment characteristics in different tectonic periods are significantly different from those in the basin and other areas [22–24]. However, currently, research on the origin of trace elements in coal from the western margin of the Ordos Basin is limited. This paper investigates Carboniferous–Permian coal samples from the western edge of the Ordos Basin to explore the factors influencing the enrichment of trace elements in this region's coal, which has important scientific significance for the study of trace element enrichment mechanism; moreover, the research also has significant economic and practical value for exploring and exploiting coal measure mineral resources.

2. Geological Setting

The western margin of the Ordos Basin borders the Alxa block; Ordos Basin in the east, the Tianshan-Xingmeng collision zone in the north; and the Qinling, Qinqi, and Kunlun collision zones in the south [25]. As the western margin of the Ordos Basin is situated at the boundary and intersection of the Qinling-Qinqi orogenic belt and the Helan fold belt, which have undergone multi-stage extensional rifts and compression-closure activities, its tectonic activity was significantly influenced by the movements of these fold belts to the north and south, as well as the stability of the Ordos block [26,27]. Consequently, the basin's western margin exhibits highly complex structural characteristics, including various fault systems, folded structures, and tectonic superposition zones that evolved through different geological periods. These characteristics are illustrated in Figure 1. The fold and thrust belt on the western margin of the Ordos Basin is a prominent intracontinental fold-thrust tectonic zone in China, marking the junction between the eastern and western tectonic domains of northern China. Over multiple tectonic stages, including those related to the Indo-China, Yanshan, and Himalayan movements, folding, thrusting, and overall uplift shaped the current tectonic pattern of the basin's western margin [28,29]. The evolution of these diverse tectonic systems has a profound impact on the superposition and distribution of various sedimentary systems within the basin. As tectonic activity changes, so do the depositional environments, leading to the formation of distinct sedimentary

sequences and facies. For instance, in the Carboniferous–Permian coal-bearing stratum, the transition from confined marine sediments to continental fluvial swamp sediments reflects changes in tectonic stress and depositional conditions. Similarly, during the Mesozoic Jurassic, an important coal-forming period in the Ordos Basin, the early-to-middle Jurassic witnessed an intracontinental depression stage, characterized by inland lake, swamp, and fluvial sedimentary environments. These varying depositional environments, along with differing sediment sources and coal-forming plant communities, significantly influence the accumulation and distribution of elements in coal [30–32].

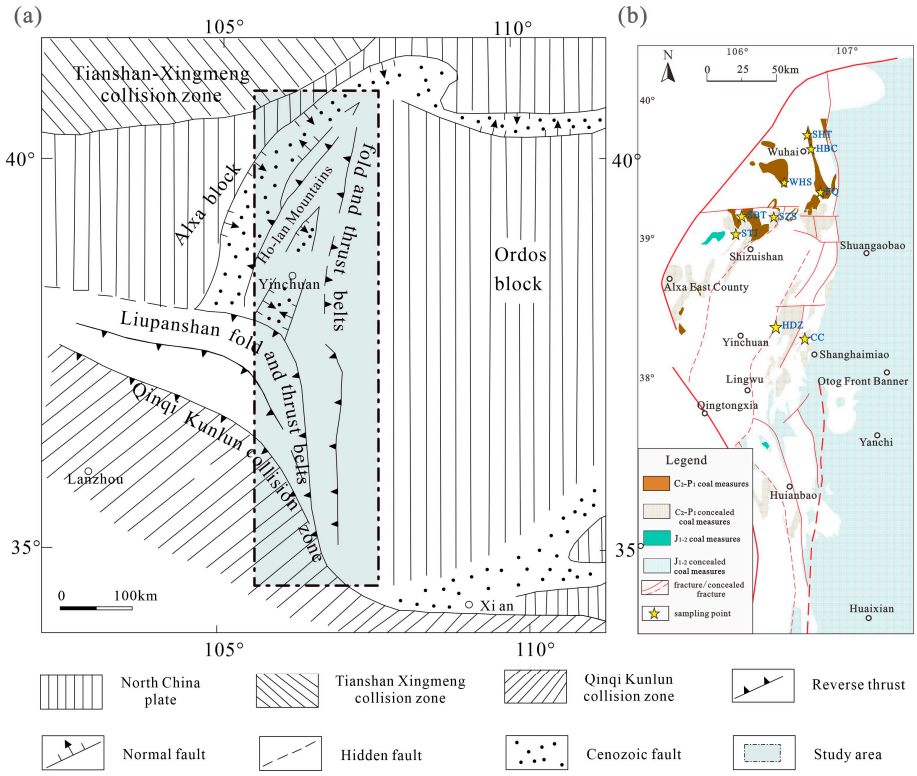

Figure 1. (**a**) Structural outline of the western margin of the Ordos Basin (modified from [24,25]); (**b**) Sampling location of western margin of Ordos Basin.

3. Sampling and Analytical Methods

Samples were collected from the Changcheng No. 1 (CC1-3, CC1-9), Changcheng No. 3 (CC3), Suhaitu (SHT), Huangbaici (HBC), Wuhushan (WHS), and Fuqiang (FQ) coal mines in the Zhuozishan coalfield; Shitanjing (STJ-5, STJ-8), Shabatai (SBT), and Shizuishan (SZS) coal mines in the Helanshan coalfield; and the Hongshiwan (HSW) and Hongdunzi (HDZ1) coal mines in the Ningdong coalfield. A total of 13 Carboniferous–Permian samples were collected (Figure 1b). Except for the samples from Fuqiang and Hongdunzi coal mines, which are carbonaceous mudstones, all other samples are coal samples.

Samples were collected following the strict guidelines of GB/T 482-2008 [33]. Moisture, volatile matter, and ash were determined according to ASTM D3173-11 (2011) [34], ASTM D3174-11 (2011) [35], and ASTM D3175-11 (2011) [36]. Total sulfur testing of coal followed ASTM D3177-02 (2007) [37]. Reflectance test of vitrinite under oil-immersed reflected light using DM4500P reflective microscope in accordance with ASTM D2798-11A (2011) [38]. The recorded reflectance values were analyzed to determine the average maximum reflectance of the vitrinite in the coal samples.

X-ray fluorescence spectroscopy (XRF; PANalytical Axios) was used to measure the concentration of major elements in samples. Preparation for XRF analysis involved borate fusion in an automated furnace, where each sample weighing 0.7 g was blended and uniformly mixed with 7 g of pure lithium borate flux, composed of 67% $Li_2B_4O_7$ and

33% $LiBO_2$. For the determination of trace elements, inductively coupled plasma mass spectrometry (ICP-MS, ELEMENT XR) was employed. These analyses were carried out in accordance with the methods described by Qin et al. [39,40] and Dai et al. [41]. These analytical techniques were conducted at the China National Nuclear Corporation (CNNC) Beijing Research Institute of Uranium Geology.

4. Results

4.1. Coal Chemistry

According to GB/T15224.1-2018 [42], STJ-5 has the lowest ash content (6.41%), which is an ultra-low-ash coal (ash content (A), A ≤ 10%); SBT and STJ-8 are low-ash coals (10% < A ≤ 20%), and SZS has the highest ash content (21.32%) and is a medium-ash coal (20% < A ≤ 30%). The moisture content ranges from 0.35%–0.61%. According to MT/T849-2000 [43], the Helanshan coalfield is made up of low to middle to high volatile coal (17.77%–31.05%). According to GB/T 15224.2-2021, STJ-5 is a medium-sulfur coal (1.83%), and other coal mines are extremely low-sulfur coal [44]. The average maximum vitrinite reflectance in the Helanshan coalfield is 1.25% (0.83%–1.51%) (Table 1).

Table 1. The content of moisture, ash, volatile matter, sulfur, vitrinite maximum reflectance, Al_2O_3, and TiO_2 of the western margin of Ordos Basin (%).

Coalfield	Horizon	Coal	Number	M_{ad}	A_d	V_{daf}	$S_{t,d}$	$R_{o,max}$	Al_2O_3	TiO_2
Helanshan	Shanxi formation	4#	SBT	0.35	13.37	18.81	0.38	1.51	42.38	0.74
		5#	STJ-5	0.42	6.41	17.77	1.83	1.19	42.21	0.28
			SZS	1.10	21.32	31.51	0.47	0.83	49.14	1.84
	Taiyuan formation	13#	STJ-8	0.61	14.4	20.92	0.48	1.45	41.32	0.82
Zhuozishan	Shanxi formation	3#	CC1-3	1.86	38.32	41.05	0.37	0.68	40.56	1.13
			WHS	0.66	41.93	V_d 16.79	6.02	0.92	25.12	1.63
	Taiyuan formation	9#	CC3	1.48	9.11	45.86	3.87	0.62	44.06	0.24
			CC1-9	1.70	4.83	40.06	2.73	0.62	30.98	1.82
		10#	SHT	0.88	43.00	V_d 17.90	1.85	1.04	32.38	1.06
			HBC	0.39	38.29	31.17	4.42	0.98	28.72	1.27
Ningdong	Shanxi formation	5#	HSW	1.84	25.17	39.62	0.71	0.69	29.66	0.87

Notes: M, moisture; ad, air-dry basis; A, ash yield; d, dry basis; V, volatile matter; daf, dry and ash-free basis; $S_{t,d}$, total sulfur; $R_{o,max}$, maximum vitrinite reflectance.

According to GB/T15224.1-2018 [42], the ash content of CC1-9 (4.83%) and CC3 (9.11%) in Zhuozishan coalfield is ultra-low, while other coal seams belong to medium- or high-ash coal (medium ash coal: 20% < A ≤ 30%; high ash coal: 30% < A ≤ 40%). The moisture content of Zhuozishan coalfield ranges from 0.39% to 3.74%, and the volatiles range from 16.79% to 45.86%. According to GB/T 15224.2-2021 [44], WHS, CC3, and HBC are high-sulfur coals; CC1-9 and FQ are medium-high-sulfur coals; and CC1-3 is an extremely low-sulfur coal. Table 1 shows that the average maximum vitrinite reflectance of the coal in the Zhuozishan coalfield is 0.83%, with a range of 0.62% to 1.04%.

The ash and moisture contents of HSW in the Ningdong coalfield are 1.84% and 25.17%, respectively, suggesting a medium-ash coal. The volatile matter and total sulfur contents suggest HSW was a high-volatile and low-sulfur coal. The average reflectance of maximum vitrinite in the Ningdong coalfield is 0.69% (Table 1).

4.2. Trace Elements

Based on the concentration coefficients (CC) concept proposed by Dai et al. [45], the CC values of trace elements in the study area were investigated by comparing them with the average of the world's hard coals [46] and common Chinese coals [47]. Table 2 displays the trace element contents in the study area.

Table 2. Content of trace elements in the study area (μg/g, on whole-coal basis).

Coalfield	Horizon	Coal	Number	Li	Be	Sc	V	Cr	Co	Ni	Cu	Zn	Ga	Rb	Sr
Zhuozishan	Shanxi formation	3#	CC1-3	103	4.59	11.2	41.5	16.2	7.15	10.4	10.1	18.3	28.5	15	234
			WHS	59.7	3.02	13.5	94.9	63.4	15.4	25.3	22	96.6	22.6	94.4	100
	Taiyuan formation	9#	CC3	46.4	0.667	2.62	13	5.66	1.42	4.1	27.9	26.5	5.26	0.788	57.8
			CC1-9	10.4	2.51	1.87	9.77	4.31	0.945	2.64	25.2	23.6	4.57	0.544	87.6
			FQ	100	4.06	15.3	53.6	23.1	7.84	16.1	16.5	65.3	30.5	11.3	422
		10#	SHT	84.6	3.99	11.6	66	26.8	8	14	22.9	30.4	21	65.7	76.8
			HBC	92.5	3.05	15.9	103	65.1	17.5	26.5	34.8	90	25.3	95.8	106
Helanshan	Shanxi formation	4#	SBT	131	3.92	10.2	20.9	6.57	4.29	7.93	11.3	32.4	23.9	9.04	83.7
		5#	STJ-5	294	2.94	10.7	67.5	19.8	1.58	14	9.8	28.6	25	5.15	54.4
			SZS	64.6	1.54	6.61	23.6	7.14	2.35	3.92	22.7	20.7	24	3.94	389
	Taiyuan formation	13#	STJ-8	43.3	2.14	6.62	27.5	9.85	2.15	5.89	29.3	31.4	14.8	1.67	176
Ningdong	Shanxi formation	5#	HDZ1	173	7.42	15.9	57.7	16.1	1.2	7.19	11.7	10.7	27.3	9.71	51
			HSW	92.1	1.91	6.37	20.8	7.69	1.51	3.15	15.9	10.7	15.5	1.94	399
Coalfield	**Horizon**	**Coal**	**Number**	**Mo**	**In**	**Sb**	**Cs**	**Ba**	**Tl**	**Pb**	**Bi**	**Th**	**U**	**REY**	
Zhuozishan	Shanxi formation	3#	CC1-3	0.648	0.1	0.54	1.61	132	0.133	28.1	0.412	19.3	4.55	245.299	
			WHS	8.81	0.068	0.603	7.16	295	1.58	32.3	0.59	14	5.17	222.714	
	Taiyuan formation	9#	CC3	2.81	0.046	0.279	0.047	24.7	0.03	10.7	0.186	2.6	1.48	34.009	
			CC1-9	4.59	0.025	0.132	0.034	46	0.006	4.09	0.266	1.3	1.49	21.02	
			FQ	16.1	0.135	0.927	0.838	82.8	0.547	44.7	0.728	26.7	14	345.295	
		10#	SHT	3.17	0.085	0.751	5.61	189	1.84	47.2	0.354	12.8	3.98	175.616	
			HBC	5.28	0.115	0.717	8.06	306	1.78	41.7	0.97	15.3	5.82	227.136	
Helanshan	Shanxi formation	4#	SBT	0.611	0.11	0.404	1.28	110	0.093	59	0.26	12	4.88	289.925	
		5#	STJ-5	10.4	0.096	0.623	0.815	149	0.26	19.5	0.637	23	30.5	56.912	
			SZS	1.02	0.029	0.592	0.124	131	0.089	32	0.188	7.52	3.42	195.801	
	Taiyuan formation	13#	STJ-8	4.6	0.043	0.579	0.121	57.3	0.176	42.4	0.303	5.9	7.5	198.23	
Ningdong	Shanxi formation	5#	HDZ1	0.833	0.123	0.25	0.91	52.7	0.184	52	0.483	27.4	4.66	314.474	
			HSW	1.83	0.051	0.231	0.164	53.9	0.065	25.9	0.44	10.2	3.39	161.047	

Compared with the world's hard coals, in the Helanshan coalfield No. 4 coal, Li and Pb are enriched (5 < CC < 10); REY, Ga, Th, Sc, In, and U are mildly enriched (2 < CC < 5); Ni, Sb, Cr, Mo, Bi, and TI are depleted (CC < 0.5); and other elements are normal (0.5 < CC < 2). In No. 5 coal, Li is highly enriched, U is enriched; and Th, Ga, Pb, Mo, Sc, and Sr are mildly enriched. In No. 13 coal, Pb, U, Li, REY, Ga, and Mo are mildly enriched; Ba, Co, Ni, Tl, Bi, Cs, and Rb are depleted; and the other elements are normal (Figure 2a).

Compared with the common Chinese coals, in the Helanshan coalfield No. 4 coal, Li, Pb, Ga, In, Sc, REY, Th, and U are mildly enriched; Sb, Cr, Bi, Mo and TI are depleted; and the other elements are normal. In No. 5 coal, U and Li are enriched; Ga and Th are mildly enriched; and other elements are normal or depleted. In No. 13 coal, U, Pb, and Ga are mildly enriched; Ni, Bi, Tl, Ba, Co, Rb, and Cs are depleted; and other elements are normal (Figure 2b).

Compared with the world's hard coals, in the Zhuozishan coalfield No. 3 coal, Li and Th are enriched; Ga, Cs, REY, Pb, Sc, Rb, U, V, Cr, Mo, In, and Zn are mildly enriched; and Bi is depleted. In No. 9 coal, Li, Mo, Th, U, Ga, and Pb are mildly enriched, while other elements are normal or depleted. In No. 10 coal, Li and Cs are enriched; and Pb, Rb, Th, Ga, Sc, Tl, V, REY, Cr, U, In, Zn, Co, and Mo are mildly enriched; and other elements are normal (Figure 3a).

Compared with the common Chinese coals, in the Zhuozishan coalfield No. 3 coal, Rb is enriched; Ga, Cs, Th, Sc, Cr, Li, Pb, and U are mildly enriched; and other elements are normal. In No. 9 coal, Mo, U, and Ga are mildly enriched; Bi, Co, Rb, Tl, Ba, and Cs are depleted. In No. 10 coal, Rb and Cs are enriched; and Tl, Ga, Sc, Cr, Pb, Li, V, Th, In, and U are mildly enriched (Figure 3b).

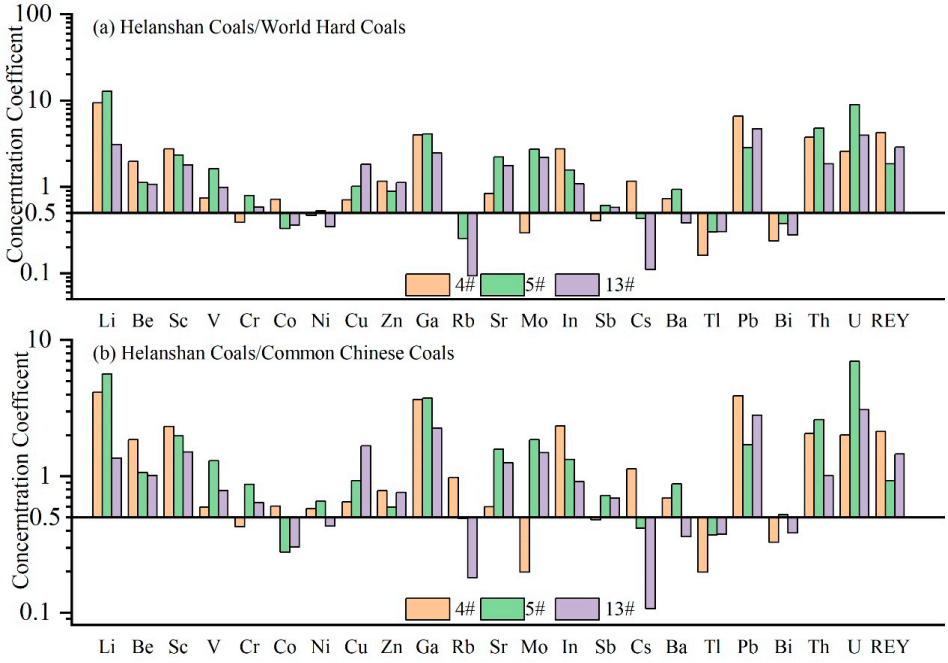

Figure 2. Trace element CC in the Helanshan coalfield; (**a**) Helanshan coalfield No. 4 coal, No. 5 coal, No. 13 coal/common world coals; (**b**) Helanshan coalfield No. 4 coal, No. 5 coal, No. 13 coal/common Chinese coals.

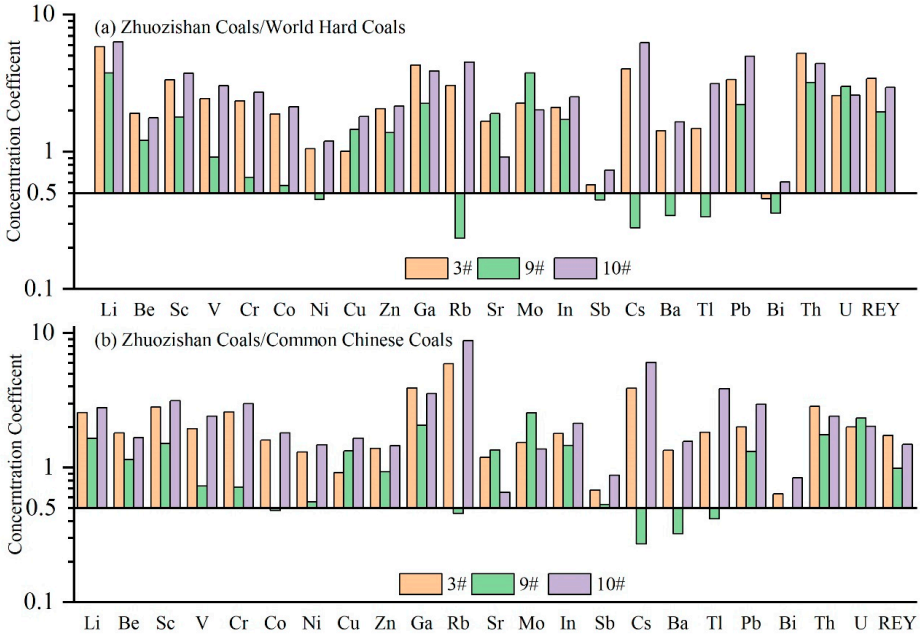

Figure 3. Trace element CC in the Zhuozishan coalfield. (**a**) Zhuozishan coalfield No. 3 coal, No. 9 coal, No. 10 coal/common world coals. (**b**) Helanshan coalfield No. 3 coal, No. 9 coal, No. 10 coal/common Chinese coals.

Compared with the world's hard coals, in the Ningdong coalfield No. 5 coal, Li and Th are enriched; Pb, Ga, REY, Sc, Be, Sr, In, and U are mildly enriched; V, Cu, Cr, and Mo are normal; and other elements are depleted (Figure 4a).

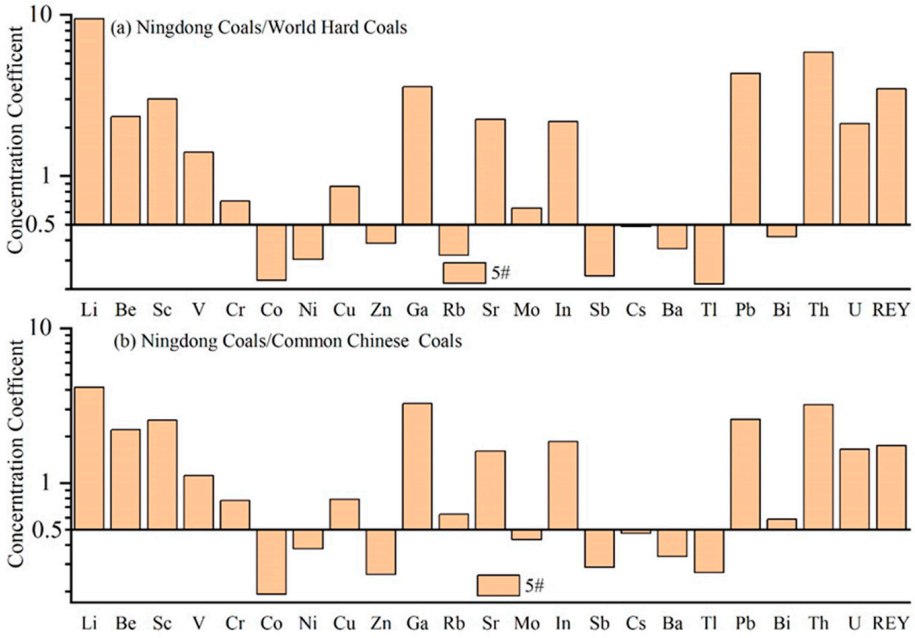

Figure 4. Trace element CC in the Ningdong coalfield; (**a**) Ningdong coalfield No. 5 coal/common world coals; (**b**) Ningdong coalfield No. 5 coal/common Chinese coals.

Compared with the common Chinese coals, in the Ningdong coalfield No. 5 coal, Li, Ga, Th, Pb, Sc, and Be are mildly enriched; In, REY, U, Sr, V, Cu, Cr, Rb, and Bi are normal; and other elements are depleted (Figure 4b).

5. Discussion

This study shows that many trace elements, such as Li and Ga, are mildly enriched or enriched in comparison with both the world's hard coals and the common Chinese coals. Recognizing the mechanism accountable for such enrichment is vital for the exploration of these critical metallic mineral resources. In this section, factors controlling trace element variations in the western Ordos Basin are first identified, followed by a discussion on the complex geological genesis of the enrichment of these trace elements.

5.1. Sediment Source

(1) Firstly, the Al_2O_3/TiO_2 ratio in coal indicates that the sediment source of trace elements in the coal of the study area is mainly intermediate and felsic igneous rocks ($Al_2O_3/TiO_2 > 8$, Figure 5a). According to the total rare earth elements to La/Yb ratio, most samples lie in the intersection area of sedimentary rock, alkaline basalt, and granite (Figure 5b). However, CC3, CC1-9, and STJ-5 fall within the sedimentary rock area, suggesting a relatively simple source for these samples, mainly sedimentary rock (calcareous mudstone). The sediment source for other samples in the study area is quite complex, consisting of a mix of granite, alkaline basalt, and sedimentary rock [48–50]. The mixed origin of sediment source components also causes the ash content of other samples to be significantly higher than that of CC3, CC1-9, and STJ in the study area (Figure 6).

(2) Secondly, the ancient strata and crystalline basement around the Ordos Basin mainly consist of ancient metamorphic rocks, including various volcanic and sedimentary rocks from Archean Eonothem and Proterozoic Eonothem [51]. In the late Paleozoic Era, the Alxa block and the Yinshan oldland were uplifted, directing the paleowater flow in the western margin of the basin from north to south or northwest to southeast, which made it possible for the Yinshan oldland and the Alxa oldland to provide provenance supply for the study area [52]. Since the terrigenous area in the north and northwest of the basin did not experience a single arching uplift during its formation

but with the continuous occurrence and intensification of the collision orogeny on the north side during the uplift, the rock thrust and folding occurred in the erosion source area, which resulted in the emergence of Archean ancient metamorphic rocks and pre-intrusive granites due to tectonic changes. It forms the sediment source in the basin together with the Sinian quartzite layer, which leads to the phenomenon of mixed source in most samples in the west margin of the basin [53].

(3) According to (1) and (2), the sediment source in the study area can be basically defined, so did the provenance component cause the concentration of trace elements in coal? Figures 6 and 7 show that the vertical variation of Li, Th, U, Ga, Pb, and REY elements in coal is similar to that of A_d, except for Helanshan coalfield. They are as follows: in the Ningdong coalfield, the content of HDZ1 is obviously higher than that of HSW; and in the Zhouzishan coalfield, the ash content and elements Li, Th, U, U, Ga, Pb, and REY in CC1-3 coal are significantly higher than those in CC1-9 and CC3 coal seams, and the highest values are found in FQ. The vertical distribution characteristics of ash and trace elements indicate that sediment source is the main factor controlling trace element enrichment in the Zhuozishan and Ningdong coalfields.

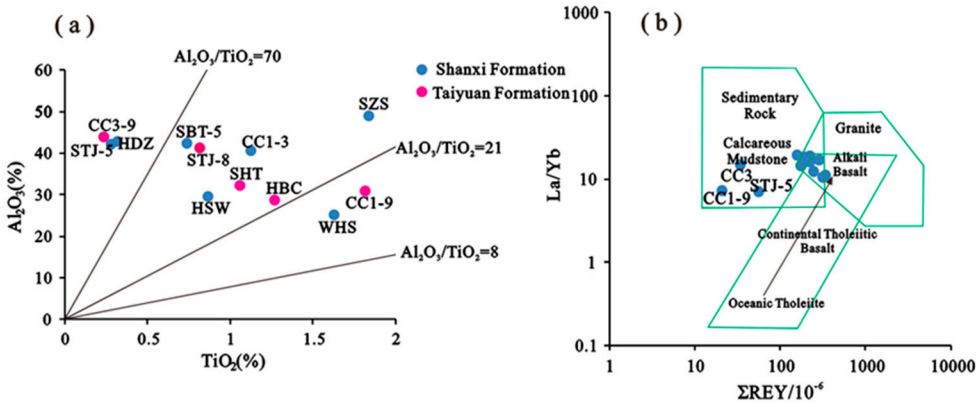

Figure 5. Relations between (**a**) Al_2O_3-TiO_2; (**b**) La/Yb-∑REY for coals in western Ordos Basin.

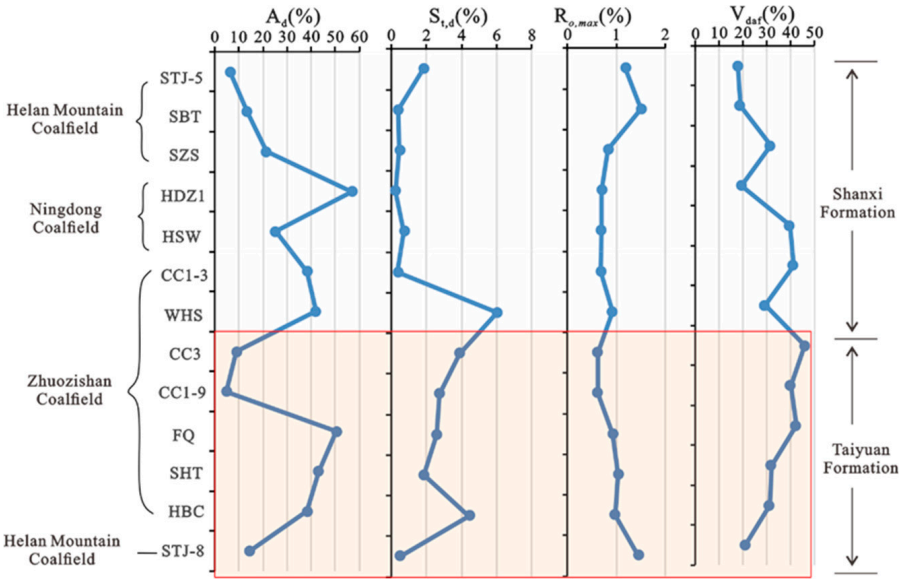

Figure 6. Variation of ash, total sulfur, volatile components, and Ro in coal.

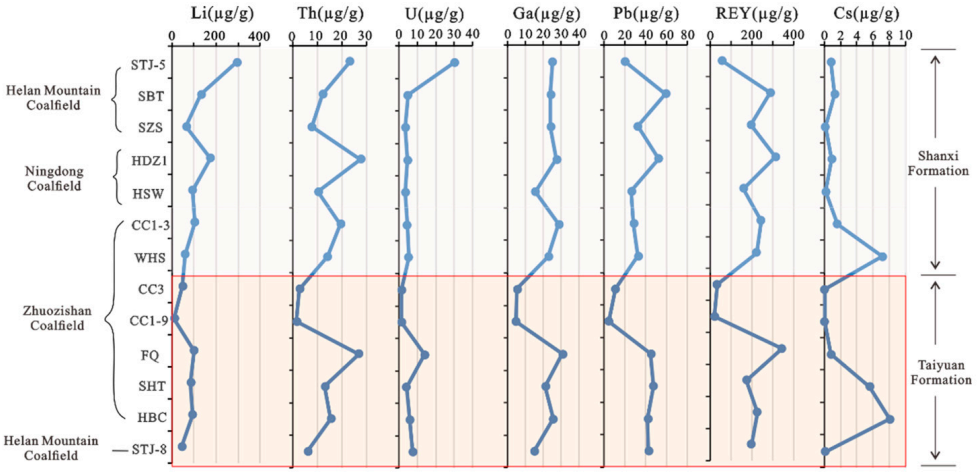

Figure 7. Variation of Li, Th, U, Ga, Pb, REY, and Cs in coal.

The variation trend of Li, Th, U, Ga, Pb, and REY elements in the Helanshan coalfield coal differs from that of A_d. This indicates that the high concentration of these elements is likely due to factors such as structural-hydrothermal processes and coal metamorphism rank, rather than sediment source composition (discussed in detail below).

(4) The distribution patterns of rare earth elements in most samples (except STJ-5 coal in Helanshan coalfield, Figure 8b) show an enrichment of light-rare earth elements or medium-rare earth elements (Figure 8a). Research indicates that intermediate and felsic igneous rocks exhibit a light rare earth element enrichment pattern, whereas mixed lithologies, such as alkaline basalt, can lead to heavy rare earth element enrichment in some samples [54], which is consistent with the above inference.

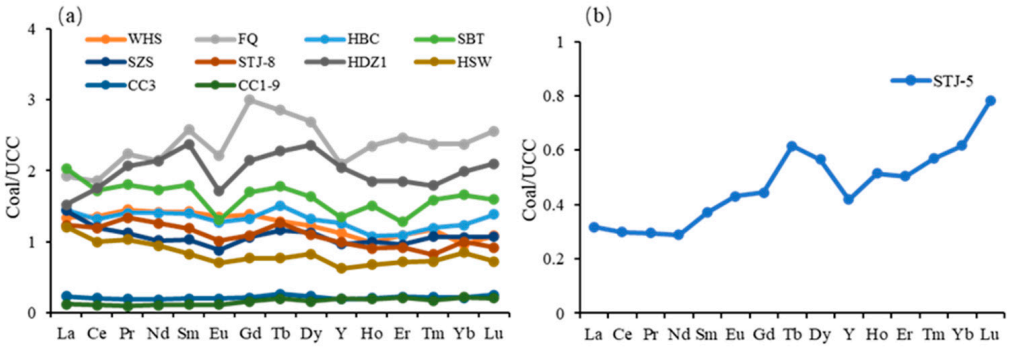

Figure 8. Distribution pattern of rare earth elements in coal (**a**) enrichment of light-rare earth elements or light-to-medium-rare earth elements; (**b**) enrichment of heavy-rare earth elements.

5.2. Fault Structure-Low Temperature Hydrothermal Fluid-Coal Metamorphism

As can be seen from the above, the accumulation of trace elements in the Zhuozishan coalfield and Ningdong coalfield is mainly controlled by the source supply, while the low concentration of ash in the Helanshan coalfield and the correlation between trace element content and low ash content indicate that the high concentration of trace elements in the Helanshan coals is not attributed to the sediment source.

The trend of ash content in coal from STJ-5 coal seam in the Shitanjing mining area of the Helanshan coalfield, which is low (6.41%), resembles that of CC1-9 and CC3 in the Shanghaimiao mining area of the Zhuozishan coalfield (4.83% and 9.11%, respectively), suggesting similar limited source sediment material supply. However, despite this similarity in ash content, the concentration of trace elements in STJ-5 exhibits a notably higher trend, such as Li (294 μg/g), Th (23 μg/g), and U (30.5 μg/g) compared to CC1-9 and CC3, and also exceeds those in other mines in Helanshan. There must be other factors

contributing to the increased elemental content in the Shitanjing coal. Through mineralogical analysis, it was discovered that fracture-filling pyrite is widespread in STJ-5 of the Shitanjing coal mine (Figure 9), indicating the intrusion of sulfur-bearing hydrothermal fluids either during the initial stages of No. 5 coal formation or post-coal formation. The main structural feature of the Helanshan coalfield is the Helanshan syncline, within which there are several major fault structures. Most of the coal mining areas in the Helanshan coalfield are located within folds trending north-northeast (or north-northwest) of the Helanshan syncline, accompanied by high-angle thrust faults that are mainly pushed from west to east [55]. These developed fault structures provide channels for sulfur-bearing fluids. As these fluids flow, they capture a variety of trace elements from the surrounding rock, enriching them with abundant Li, Th, U, and other elements. Coal, being a porous medium with developed fractures, facilitates rapid pressure drops and the unloading of the fluids, leading to the precipitation and enrichment of minerals and elements. This results in the secondary enrichment of Li, Th, U, and other elements in STJ-5 of the Shitanjing mine, significantly increasing their concentrations compared to those in coals from other mines in the Helanshan coalfield. Additionally, the input of these hydrothermal fluids is a crucial factor contributing to the heavy rare earth element distribution pattern observed in STJ-5 of the Helanshan coalfield (Figure 8b) [56].

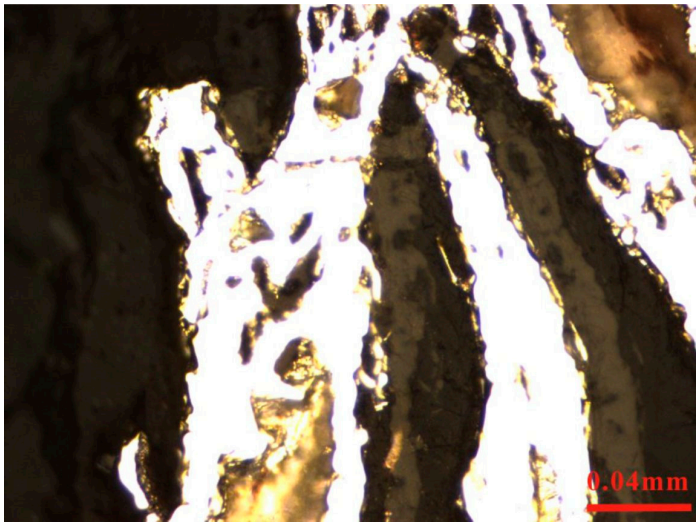

Figure 9. Fracture-filling pyrite, sample STJ-5, observed under an optical microscope.

The near-north-south compressive tectonic stress field of the Indosinian period gradually transitioned to the near-east-west compressive stress field of the Yanshan period. The Ordos Basin began to develop a tensile environment, and magmatic activity occurred in the Rujigou area, which led to the complete change of sedimentary tectonic pattern in the Ordos Basin and the transformation of the early sedimentary basin. For example, the distribution characteristics of basalt in Helanshan coalfield are from northeast to southwest to near east to west on the plane, but the thermal metamorphism of coal is not only dependent on the direct thermal contact metamorphism of magma but more importantly on the heat transfer of thermal fluid. Therefore, on the one hand, the coal metamorphism change is centered on Rujigou, and the coal grade slowly diminishes from Rujigou to the southwest and northeast. On the other hand, the metamorphism of coal is mainly closely related to the development of dikes, which causes the development height of the dikes along the fissure and the local variation of the reflectivity to the same height and also causes the heterogeneity of the metamorphism of the coal seam in a small range in the same area [57]. In addition to the influence of magmatic-hydrothermal solution, another leading factor of coal metamorphism is the thickness of the overburden layer in the Helanshan coalfield. For example, although the Shabatai area is far away from Rujigou coal, its thick Triassic strata lead to a higher metamorphism of SBT (1.51%), while STJ coal is close to Rujigou coal, but

its overburden rock series is less thick [58]. Therefore, the metamorphism degree of SBT coal exceeds that of STJ coal. The impression of temperature and the enrichment of organic matter in coal on the development of channels and coal metamorphism is significant. High temperatures can enhance the fluid mobility within the coal seams, promoting the development of channels and fractures, which in turn facilitate the migration of hydrocarbons and other fluids. Additionally, the enrichment of organic matter within the coal can influence its metamorphic degree as higher organic content often correlates with increased coal rank and altered physical and chemical properties [59–62]. The degree of coal metamorphism also influences the accumulation of trace elements in coal. Liu et al. discovered that the Ga content in sub-volcanic thermal metamorphic coal decreased with the increase of coal metamorphism [63]. The content of Ga in the coal in the Helanshan coalfield does not show an obvious relationship with the degree of coal metamorphism, while the variation of Pb and REY elements with the degree of metamorphism is obvious, which indicates that the relatively rich Pb and REY contents in Helanshan coalfield may be mainly controlled by the degree of coal metamorphism [18].

In low-rank coal, most trace elements can be partly linked to organic matter and partly found in minerals. Most trace elements in bituminous coal and anthracite belong to an inorganic binding state. As the coal rank increases, carboxyl and hydroxyl groups detach from the coal's macromolecular structure, resulting in a decrease in trace elements associated with these functional groups. The concentration of organically bound trace elements in lignite is relatively high, while the content in bituminous coal is reduced, and the content of organically bound trace elements in anthracite is further reduced [64,65]. Researchers have demonstrated that as coal rank increases, the organic binding states of Cr and V elements decrease, and the occurrence of these elements in minerals becomes more prominent. Additionally, trace elements bound to organic matter are more volatile than those associated with minerals [66–68]. Huggins and Huffman explored the transition from chelated organic associations in peat and low-rank coal to inorganic associations in high-volatile bituminous coal, which is found in the Illinois Basin [69]. While they demonstrated that some chromium, titanium, vanadium, and zirconium in these coals may be present as organic components, there is an overall tendency for organic binding to decrease as the coal rank increases.

5.3. Complex Geological Genesis of Trace Element Enrichment

The ancient strata and crystalline basement in the surrounding area of the Ordos Basin mainly consist of multiple sets of ancient metamorphic rock series composed of various types of volcano-sedimentary rocks of the Archean and Proterozoic Eocene [24]. The direction of ancient water in the western margin of the basin made it possible for Yinshan oldland and Alashan oldland to provide a provenance supply to the study area in the late Paleozoic [70]. While the terrigenous area in the north and northwest of the basin was uplifted during the formation process, the collision orogeny on the north side and the intensification of the erosion source area resulted in the thrusts and folds of the rock layers. As a result, the Archean ancient metamorphic rock and the granites that invaded earlier emerged from the surface due to tectonic changes, which together with the Sinian quartzite layer constituted the sediment source in the basin. The provenance of most coal mines in the western margin of the basin is a mixed lithology of granite, alkaline basalt, and sedimentary rock [53]. Only the provenance of CC1-9, CC3, and STJ-5 coal is relatively simple, mainly sedimentary rock (calcareous mudstone).

The above multiple sediment source supply is the most important factor controlling the enrichment of trace elements in the Zhuozishan coalfield and the Ningdong coalfield. The mixture of granite, alkaline basalt, and sedimentary rock from the Yinshan and Alxa oldlands makes the ash content in Zhuozishan and Ningdong coalfields relatively high. Moreover, the vertical variation of Li, Th, U, Ga, Pb, and REY elements and ash content in coal is basically the same. The distribution patterns of rare earth elements in coal are light rare earth element enrichment or medium rare earth element enrichment.

During the Carboniferous–Permian period, the Helanshan coalfield experienced frequent tectonic activities. These activities included crustal movements, fault formations, and uplift and subsidence of the strata. The crustal movements were particularly intense, leading to significant changes in the geological structure of the coalfield. Faults developed extensively throughout the region, disrupting the continuity of coal seams and causing significant displacement and deformation of the coal-bearing strata. These frequent structural changes disrupted the stability of the surface, exposed rocks to erosion, and reduced the available depositional space, ultimately resulting in a limited source material supply [71–73]. As a result, the total ash content of some coal mines in the Helanshan coalfield is obviously lower than that in the Zhuozishan coalfield and the Ningdong coalfield, with the content of the former ranging from 13.37% to 21.32%. The contents of the latter ranged from 38.29%–50.57% and 25.17%–57.02%. Therefore, the sediment source did not cause the enrichment of trace elements in the coal in the Helanshan coalfield. The variation trend of Li, Th, U, Ga, Pb, and REY elements in coal in this area is quite different from that of A_d.

The fault structure of the Helanshan coalfield provided a channel for hydrothermal fluids. When sulfur-containing hydrothermal fluids invaded STJ-5 coal along the fissure, pyrite-bearing veins were widely developed in the coal, and the hydrothermal fluids captured a variety of trace elements from the surrounding rock, thus carrying abundant Li, Th, U, and other elements. Due to the characteristics of coal fissure development, the fluid pressure drops sharply and is quickly unloaded. This results in the precipitation and enrichment of minerals and elements in the fluid, resulting in the content of Li, Th, U, and other elements in STJ-5 coal being significantly higher than other coal mines in the Helanshan coalfield. In addition, the input of sulfur-containing hydrothermal fluid leads to the distribution pattern of heavy rare earth elements in STJ-5 in the Helanshan coalfield, and the total sulfur content is as high as 1.83%, which is 3.8–4.8 times that of other Taiyuan formation coal seams in the Helanshan coalfield.

The change of compressive tectonic stress field near south to north in the Indosinian period led to the emergence of a tensile environment in the Ordos Basin, and the magmatic activity in Rujigou in some parts of the Ordos Basin led to a radical change in the sedimentary tectonic pattern of the Ordos Basin and a transformation of the sediments in the earlier basin [74]. The rank of the coal metamorphism of Carboniferous–Permian coal in the Helanshan coalfield is generally higher than that of other coal mines (0.83%–1.51%) due to the influence of magmatic heat. Lead and REY elements in the Helanshan coalfield show similar changes to R_o, and the opposite changes to volatilization are affected by the rank of coal metamorphism. As the rank of coal metamorphism increased, decarboxylation and removal of other oxygen-containing functional groups resulted in a reduction in metal–COOM bonds, and the released metals can be synthesized into clays and other minerals. Additionally, as the water content decreased, the cation-containing solution became saturated, and if separated from the clay, the cations formed hydroxides or oxides [75].

In summary, on the basis of revealing the response of coal geochemical characteristics to the geological evolution of the basin, a composite genetic model of provenance—fault structure—low-temperature hydrothermal fluid—coal metamorphism of trace elements in Carboniferous–Permian coal in the western margin of Ordos Basin has been established (Figure 10). In this model, folds and faults are very developed. Although the provenance may provide enough debris sources for the study area due to frequent structural changes and the loss of debris supply due to denudation or erosion, the provenance does not ultimately cause the enrichment of elements. The widely developed fault structures provided channels for sulfur-containing hydrothermal fluids, and the increase in the degree of coal metamorphism eventually resulted in the enrichment of elements in the present coal in the study area.

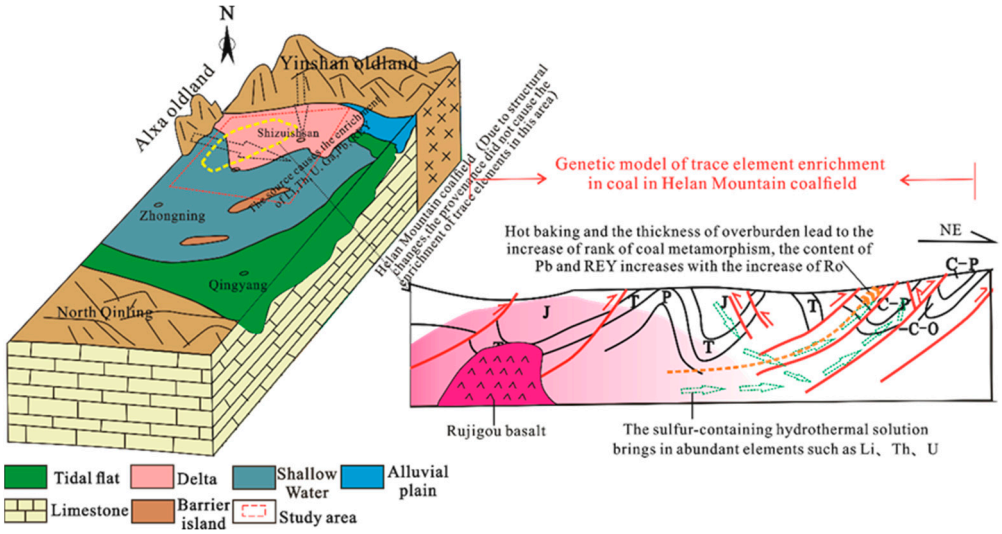

Figure 10. Composite genetic model dominated by provenance—fault structure—low-temperature hydrothermal fluid—coal metamorphism. The red dotted line represents "Hot baking and the thickness of overburden lead to the increase of rank of coal metamorphism".

6. Conclusions

(1) The coal in the Helanshan coalfield is classified as ultra-low to medium ash and ultra-low- to medium-sulfur coal, and the metamorphism degree of coal varies greatly, $R_{o,max}$ is 0.83%–1.51%, with an average value of 1.25%, which is higher than $R_{o,max}$ of coals in Ningdong and Zhuozishan coalfields.

(2) Compared with the world average, Li and Th are concentrated in No. 3 coal of the Zhuozishan coalfield, while Li and Cs are concentrated in No. 10 coal. The enrichment of these trace elements in the Zhuozishan coalfield was mainly attributed to the provenance. In the Helanshan coalfield, the enrichment of Li and Pb in No. 4 coal, and the high enrichment of Li in the No. 5 coal seam can be explained by the influence of fault structure, low-temperature hydrothermal fluid, and coal metamorphism.

(3) Based on the revelation of how coal geochemical characteristics respond to the geological evolution of the basin, a composite genetic model of provenance—fault structure—low-temperature hydrothermal fluid—coal metamorphism of trace elements in Carboniferous–Permian coal in the western margin of the Ordos Basin has been established. In this model, folds and faults were very developed, and the mixture of granite, alkaline basalt and sedimentary rock from the Yinshan and Alxa oldlands caused the relative enrichment of Li, Th, U, Ga, Pb, and REY elements in the Zhuozishan and Ningdong coalfields, but the source supply did not lead to the enrichment of trace elements in the tectonically active Helanshan coalfield. The primary reason for the accumulation of trace elements in the Helanshan coalfield is the widespread development of fault structures, which served as channels for sulfur-containing hydrothermal fluids and influenced the degree of coal metamorphism. Additionally, temperature plays a significant role in this process, which can enhance the fluid mobility within the coal seams, promoting the development of channels and fractures, which in turn facilitate the migration of hydrocarbons and other fluids. In addition, Temperature also affects coal metamorphism, which can affect the solubility and adsorption capacity of trace elements, further influencing their distribution and enrichment in Helanshan coals.

Author Contributions: Data curation, G.Q. and Y.S.; formal analysis, Y.S. and G.Q.; methodology, S.L., X.D., W.C., W.S. and Y.Z.; resources, G.Q.; supervision, G.Q.; writing—original draft, G.Q., Y.S. and K.S. All authors have read and agreed to the published version of the manuscript.

Funding: This work was funded by the National Natural Science Foundation of China (42202197 and 42372187), the Science Research Project of Hebei Education Department (BJK2024073), and the funding project of Northeast Geological S&T Innovation Center of China Geological Survey (NO. QCJJ2023-02).

Data Availability Statement: Data is available upon request due to restrictions.

Conflicts of Interest: The authors declare no conflicts of interest.

References

1. Seredin, V.V. From coal science to metal production and environmental protection: A new story of success. *Int. J. Coal Geol.* **2012**, *90*, 1–3. [CrossRef]
2. Seredin, V.V.; Dai, S.; Sun, Y.; Chekryzhov, I.Y. Coal deposits as promising sources of rare metals for alternative power and energy-efficient technologies. *Appl. Geochem.* **2013**, *31*, 1–11. [CrossRef]
3. Dai, S.; Finkelman, R.B. Coal as a promising source of critical elements: Progress and future prospects. *Int. J. Coal Geol.* **2018**, *186*, 155–164. [CrossRef]
4. Dai, S.; Arbuzov, S.I.; Chekryzhov, I.Y.; French, D.; Feole, I.; Folkedah, B.C.; Graham, I.T.; Hower, J.C.; Nechaev, V.P.; Wagner, N.J.; et al. Metalliferous coals of Cretaceous age: A review. *Minerals* **2022**, *12*, 1154. [CrossRef]
5. Dai, S.; Ren, D.; Chou, C.L.; Li, S.; Jiang, Y. Mineralogy and geochemistry of the No. 6 Coal (Pennsylvanian) in the Junger Coalfield, Ordos Basin, China. *Int. J. Coal Geol.* **2006**, *66*, 253–270. [CrossRef]
6. Dai, S.; Li, D.; Chou, C.L.; Zhao, L.; Zhang, Y.; Ren, D.; Ma, Y.; Sun, Y. Mineralogy and geochemistry of boehmite-rich coals: New insights from the Haerwusu Surface Mine, Jungar Coalfield, Inner Mongolia, China. *Int. J. Coal Geol.* **2008**, *74*, 185–202. [CrossRef]
7. Sun, Y.; Zhao, C.; Qin, S.; Xiao, L.; Li, Z.; Lin, M. Occurrence of some valuable elements in the unique 'high-aluminium coals' from the Jungar coalfield, China. *Ore Geol. Rev.* **2016**, *72*, 659–668. [CrossRef]
8. Sun, Y.; Zhao, C.; Li, Y.; Wang, J.; Zhang, J.; Jin, Z.; Lin, M.; Wolfgang, K. Further information of the associated Li deposits in the No.6 Coal Seam at Jungar Coalfield, Inner Mongolia, Northern China. *Acta Geol. Sin.* **2013**, *87*, 1097–1108.
9. Sun, Y.; Zhao, C.; Zhang, J.; Yang, J.; Zhang, Y.; Yuan, Y.; Duan, D. Concentrations of valuable elements of the coals from the Pingshuo Mining District, Ningwu Coalfield, northern China. *Energy Explor. Exploit.* **2013**, *31*, 727–744. [CrossRef]
10. Qin, G.; Liu, K.; Xu, H.; Ma, Z.; Deng, L.; Cao, D. Paragenetic Association Features of Trace Elements in Coals in Western Margin of Ordos Basin. *Coal Geol. China* **2015**, *27*, 1–6+18. (In Chinese)
11. Yi, T.; Qin, Y.; Wu, Y.; Li, Z. Gallium accumulation and geological controls in coal seam and its floor from Liangshan Formation, Kaili, Eastern Guizhou, China. *J. China Univ. Min. Technol.* **2007**, *3*, 330–334. (In Chinese)
12. Li, S.; Ren, D. Analysis of anomalous high concentration of lead and selenium and their origin in the main minable coal seam in the Junger Coalfield. *J. China Univ. Min. Technol.* **2006**, *5*, 612–616. (In Chinese)
13. Zhu, H.; Huang, C.; Ju, Y.; Bu, H.; Li, X.; Yang, M.; Chu, Q.; Feng, H.; Qiao, P.; Qi, Y.; et al. Multi-scale multidimensional characterization of clay-hosted pore networks of shale using FIBSEM, TEM, and X-ray micro-tomography: Implications for methane storage and migration. *Appl. Clay Sci.* **2021**, *213*, 106239. [CrossRef]
14. Dai, S.; Yan, X.; Ward, C.; Hower, J.; Zhao, L.; Wang, X.; Zhao, L.; Ren, D.; Finkelman, R. Valuable elements in Chinese coals: A review. *Coal Geol. China* **2018**, *60*, 590–620. [CrossRef]
15. Wang, X.; Dai, S.; Ren, D.; Yang, J. Mineralogy and geochemistry of Al-hydroxide/oxyhydroxide mineral-bearing coals of Late Paleozoic age from the Weibei coalfield, southeastern Ordos Basin, North China. *Appl. Geochem.* **2011**, *26*, 1086–1096. [CrossRef]
16. Shen, Y.; Guo, Y.; Li, Z.; Wei, X.; Xue, L.; Liu, J. Distribution of radioactive elements (U, Th) in the upper Paleozoic coal-bearing strata of the eastern Ordos basin. *J. Pet. Sci. Eng.* **2017**, *157*, 1130–1142. [CrossRef]
17. Dai, S.; Jiang, Y.; Ward, C.R.; Gu, L.; Seredin, V.V.; Liu, H.; Zhou, D.; Wang, X.; Sun, Y.; Zou, J.; et al. Mineralogical and geochemical compositions the coal in the Guanbanwusu Mine, Inner Mongolia, China: Further evidence for the existence of an Al (Ga and REE) ore deposit in the Jungar Coalfield. *Int. J. Coal Geol.* **2012**, *98*, 10–40. [CrossRef]
18. Qin, G. Enrichment Characteristics and Genetic Types of Trace Elements in the Late Paleozoic Coal from Ordos Basin. Ph.D. Thesis, China University of Mining and Technology-Beijing, Beijing, China, 2024. (In Chinese).
19. Sun, Y.; Zhao, C.; Li, Y.; Wang, J.; Liu, S. Li distribution and mode of occurrences in Li-bearing coal seam 6 from the Guanbanwusu Mine, Inner Mongolia, Northern China. *Energy Explor. Exploit.* **2012**, *30*, 109–130. [CrossRef]
20. Li, J.; Zhuang, X.; Wei, Y.; Liu, B.; Querol, X.; Font, O.; Moreno, N.; Li, J.; Gang, T.; Liang, G. Mineral composition and geochemical characteristics of the Li-Ga-rich coals in the Buertaohai-Tianjiashipan mining district, Jungar Coalfield, Inner Mongolia. *Int. J. Coal Geol.* **2016**, *167*, 157–175. [CrossRef]
21. Qin, G.; Cao, D.; Wei, Y.; Wang, A.; Liu, J. Geochemical characteristics of the Permian coals in the Junger-Hebaopian mining district, northeastern Ordos Basin, China: Key role of paleopeat-forming environments in Ga-Li-REY enrichment. *J. Geochem. Explor.* **2020**, *213*, 106494. [CrossRef]
22. Sun, J.; Dong, Y. Middle–Late Triassic sedimentation in the Helanshan tectonic belt: Constrain on the tectono-sedimentary evolution of the Ordos Basin, North China. *Geosci. Front.* **2019**, *10*, 213–227. [CrossRef]
23. Wang, L.; Jiang, B.; Wang, J.; Qu, Z.; Chen, R. Structural controls on joint development in the southeastern margin of the Ordos basin. *Arab. J. Geosci.* **2016**, *9*, 352. [CrossRef]

24. Bao, H.; Huang, Z.; Guo, W.; Wang, Q.; Jing, X.; Wang, G.; Liu, J. The formation environment, hydrocarbon generating organisms, rock and mineral characteristics of the Middle-Upper Ordovician source rock layers in west margin of Ordos Basin. *Chin. J. Geol.* **2024**, *59*, 696–711. (In Chinese)
25. Liu, C.; Zhao, H.; Wang, F.; Chen, H. Attributes of the Mesozoic Structure on the West Margin of the Ordos Basin. *Acta Geol. Sin.* **2005**, *6*, 737–747. (In Chinese)
26. Liu, H.; Lu, X.; Wang, Y. *Formation and Deformation of Thrust Fold Belt in the Western Margin of Ordos*; Yang, J., Ed.; Gansu Science and Technology Press: Gansu, China, 1990; pp. 54–75. (In Chinese)
27. Guo, Q.; Li, Z.; Yu, J.; Li, X. Meso-Neozoic structural evolution in the western margin of Ordos basin with respect to uranium ore formation. *Uranium Geol.* **2010**, *26*, 137–143. (In Chinese)
28. Ritts, B.D.; Weislogel, A.; Graham, S.A.; Darby, B.J. Mesozoic Tectonics and Sedimentation of the Giant Polyphase Nonmarine Intraplate Ordos Basin, Western North China Block. *Int. Geol. Rev.* **2009**, *51*, 95–115. [CrossRef]
29. Li, R.; Li, Y. Tectonic evolution of the western margin of the Ordos Basin (Central China). *Russ. Geol. Geophys.* **2008**, *49*, 23–27.
30. Rimmer, S.M. Geochemical paleoredox indicators in Devonian-Mississippian black shales, Central Appalachian Basin (USA). *Chem. Geol.* **2004**, *206*, 373–391. [CrossRef]
31. Scheffler, K.; Buehmann, D.; Schwark, L. Analysis of late Palaeozoic glacial to postglacial sedimentary successions in South Africa by geochemical proxies—Response to climate evolution and sedimentary environment. *Palaeogeogr. Palaeoclimatol. Palaeoecol.* **2006**, *240*, 184–203. [CrossRef]
32. Dai, S.; Li, T.; Jiang, Y.; Ward, C.R.; Hower, J.C.; Sun, J.; Liu, J.; Song, H.; Wei, J.; Li, Q.; et al. Mineralogical and geochemical compositions of the Pennsylvanian coal in the Hailiushu Mine, Daqingshan Coalfield, Inner Mongolia, China: Implications of sediment-source region and acid hydrothermal solutions. *Int. J. Coal Geol.* **2015**, *137*, 92–110. [CrossRef]
33. *Chinese National Standard GB/T 482-2008*; Standardization Administration of China; Sampling of Coal Seams. Standard Press of China: Beijing, China, 2008. (In Chinese)
34. *ASTM Standard D3173-11*; Test Method for Moisture in the Analysis Sample of Coal and Coke. ASTM International: West Conshohocken, PA, USA, 2011.
35. *ASTM Standard D3174-11*; Annual Book of ASTM Standards. Test Method for Ash in the Analysis Sample of Coal and Coke. ASTM International: West Conshohocken, PA, USA, 2011.
36. *ASTM Standard D3175-11*; Test Method for Volatile Matter in the Analysis Sample of Coal and Coke. ASTM International: West Conshohocken, PA, USA, 2011.
37. *ASTM Standard D3177-02*; Standard Test Methods for Total Sulfur in the Analysis Sample of Coal and Coke (Withdrawn 2012). ASTM International: West Conshohocken, PA, USA, 2007.
38. *ASTM Standard D2798-11A*; Standard Test Method for Microscopical Determination of the Vitrinite Reflectance of Coal. ASTM International: West Conshohocken, PA, USA, 2011.
39. Qin, G.; Cao, D.; Wei, Y.; Wang, A.; Liu, J. Mineralogy and Geochemistry of the No. 5^{-2} High-Sulfur Coal from the Dongpo Mine, Weibei Coalfield, Shaanxi, North China, with Emphasis on Anomalies of Gallium and Lithium. *Minerals* **2019**, *9*, 402. [CrossRef]
40. Qin, G.; Wei, J.; Wei, Y.; Cao, D.; Li, X.; Zhang, Y. The Differences in the Li Enrichment Mechanism between the No. 6 Li-Rich Coals and Parting in Haerwusu Mine, Ordos Basin: Evidenced Using In Situ Li Microscale Characteristics and Li Isotopes. *Minerals* **2024**, *14*, 836. [CrossRef]
41. Dai, S.; Wang, X.; Zhou, Y.; Hower, J.C.; Li, D.; Chen, W.; Zhu, X. Chemical and mineralogical compositions of silicic, mafic, and alkali tonsteins in the late Permian coals from the Songzao Coalfield, Chongqing, Southwest China. *Chem. Geol.* **2011**, *282*, 29–44. [CrossRef]
42. *Chinese National Standard GB/T 15224.1-2018*; Standardization Administration of China. Classification for Quality of Coal—Part 1: Ash. Standard Press of China: Beijing, China, 2018. (In Chinese)
43. *Chinese National Standard MT/T849-2000*; Standardization Administration of China. Classification for Volatile Matter of Coal. Standard Press of China: Beijing, China, 2000. (In Chinese)
44. *Chinese National Standard GB/T 15224.2-2021*; Standardization Administration of China. Classification for Quality of Coal—Part 2: Sulfur Content. Standard Press of China: Beijing, China, 2021. (In Chinese)
45. Dai, S.; Seredin, V.V.; Ward, C.R.; Hower, J.C.; Xing, Y.; Zhang, W.; Song, W.; Wang, P. Enrichment of U-Se-Mo-Re-Vin coals preserved within marine carbonate successions: Geochemical and mineralogical data from the Late Permian Guiding Coalfield, Guizhou, China. *Miner. Deposita* **2015**, *50*, 159–186. [CrossRef]
46. Ketris, M.P.; Yudovich, Y.E. Estimations of Clarkes for Carbonaceous biolithes: World averages for trace element contents in black shales and coals. *Int. J. Coal Geol.* **2009**, *78*, 135–148. [CrossRef]
47. Dai, S.; Ren, D.; Chou, C.L.; Finkelman, R.B.; Seredin, V.V.; Zhou, Y. Geochemistry of trace elements in Chinese coals: A review of abundances, genetic types, impacts on human health, and industrial utilization. *Int. J. Coal Geol.* **2012**, *94*, 3–21. [CrossRef]
48. Hayashi, K.I.; Fujisawa, H.; Holland, H.D.; Ohmoto, H. Geochemistry of ~1.9 Ga sedimentary rocks from northeastern Labrador, Canada. *Geochim. Cosmochim. Acta* **1997**, *61*, 4115–4137. [CrossRef]
49. Wei, Y.; He, W.; Qin, G.; Wang, A.; Cao, D. Mineralogy and Geochemistry of the Lower Cretaceous Coals in the Junde Mine, Hegang Coalfield, Northeastern China. *Energies* **2022**, *15*, 5078. [CrossRef]

50. Liu, J.; Nechaev, V.P.; Dai, S.; Song, H.; Nechaeva, E.V.; Jiang, Y.; Graham, L.T.; French, D.; Yang, P.; Hower, J.C. Evidence for multiple sources for inorganic components in the Tucheng coal deposit, western Guizhou, China and the lack of critical-elements. *Int. J. Coal Geol.* **2020**, *223*, 103468. [CrossRef]
51. Zhai, Y.; He, D.; Kai, B. Tectono-depositional environment and prototype basin evolution in the Ordos Basin during the Early Permian. *Earth Sci. Front.* **2023**, *30*, 139–153. (In Chinese)
52. Wang, S. Ordos Basin superposed evolution and structural controls of coal forming activities. *Earth Sci. Front.* **2017**, *24*, 54–63. (In Chinese)
53. Chen, Q.; Li, W.; Hu, X.; Li, K.; Pang, J.; Guo, Y. Tectonic Setting and Provenance Analysis of Late Paleozoic Sedimentary Rocks in the Ordos Basin. *Acta Geol. Sin.* **2012**, *86*, 1150–1162. (In Chinese)
54. Dai, S.; Graham, I.T.; Ward, C.R. A review of anomalous rare earth elements and yttrium in coal. *Int. J. Coal Geol.* **2016**, *159*, 82–95. [CrossRef]
55. Cao, D.; Wei, Y.; Qin, G.; Ning, S.; Wang, A.; Zhang, Y.; Li, X.; Wei, J.; Xu, L. Tectonic control on enrichment and metallogenesis of strategic metal elements in coal measures. *Coal Geol. Explor.* **2023**, *51*, 66–85. (In Chinese)
56. Seredin, V.V.; Dai, S. Coal deposits as potential alternative sources for lanthanides and yttrium. *Int. J. Coal Geol.* **2012**, *94*, 67–93. [CrossRef]
57. Wang, F.; Liu, C.; Yang, X.; Su, C. Geologic geochemical features of basalt in Ruqi Clough of Helan Mountain and its structural environmental significance. *Pet. Geol. Oilfield Dev. Daqing* **2005**, *4*, 25–27+6. (In Chinese)
58. Sun, J.Q. *Coal Resource Potential Evaluation Report of Helan Mountain Coalfield in Ningxia Hui Autonomous Region*; Coal Geological Bureau of Ningxia Hui Autonomous Region: Yinchuan, China, 2010. (In Chinese)
59. Scott, A.R. Hydrothermal alteration of coal: The role of temperature and time. *Int. J. Coal Geol.* **1987**, *7*, 291–311.
60. Gayer, R.A.; Harris, I. *Coalbed Methane and Coal Geology*; Geological Society: London, UK, 1996; Volume 109, pp. 65–89.
61. Laubach, S.E.; Marrett, R.A.; Olson, J.E.; Scott, A.R. Hierarchical fracture modeling in reservoir geomechanics. *Am. Assoc. Pet. Geol. Bull.* **1998**, *82*, 831–849.
62. Michiel, M.; Gallucci, E. Organic matter and mineral matter interactions in low-rank coals: An XPS and TGA/FTIR study. *Fuel* **2011**, *90*, 1860–1867.
63. Liu, J.; Xu, Y. Distribution of Ge, Ga, As, S in the coal metamorphized by heat of sub-volcanics. *Coal Geol. Explor.* **1992**, *55*, 27–32.
64. Swaine, D.J. *Trace Elements in Coal*; Butterworths: London, UK, 1990.
65. Finkelman, R.B. Trace and minor elements in coal. In *Organic Geochemistry*; Engel, M.H., Macko, S., Eds.; Plenum: New York, NY, USA, 1993; pp. 593–607.
66. Liu, Y.; Liu, G.; Qi, C.; Cheng, S.; Sun, R. Chemical speciation and combustion behavior of chromium (Cr) and vanadium (V) in coals. *Fuel* **2016**, *184*, 42–49. [CrossRef]
67. Yan, R.; Gauthier, D.; Flamant, G. Volatility and chemistry of trace elements in a coal combustor. *Fuel* **2001**, *80*, 2217–2226. [CrossRef]
68. Zhao, Y.; Zhang, J.; Zheng, C. Release and removal using sorbents of chromium from a high-Cr lignite in Shenbei coalfield, China. *Fuel* **2013**, *109*, 86–93. [CrossRef]
69. Huggins, F.E.; Huffman, G.P. How do lithophile elements occur in organic association in bituminous coals? *Int. J. Coal Geol.* **2004**, *58*, 193–204. [CrossRef]
70. Qiu, R.; Li, T.; Xiao, Q. A new model of Late Paleozoic tectonic evolution in the Alxa Block: Records from magmatic and sedimentary rocks. *Miner. Explor.* **2024**, *15*, 1–12. (In Chinese)
71. Kim, W.; Cheong, D.; Kendall, C.G.S.C. Effects of in-phase and out-of-phase sediment supply responses to tectonic movement on the sequence development in the late Tertiary Southern Ulleung Basin, East (Japan) Sea. *Comput. Geosci.* **2007**, *33*, 299–310. [CrossRef]
72. Thamó-Bozsó, E.; Kercsmár, Z.; Nádor, A. *Tectonic Control on Changes in Sediment Supply: Quaternary Alluvial Systems, Körös Sub-Basin, SE Hungary*; Geological Society: London, UK, 2002; Volume 191, pp. 37–53.
73. Zhu, H.; Lu, Y.; Pan, Y.; Qiao, P.; Raza, A.; Liu, W. Nanoscale mineralogy and organic structure characterization of shales: Insights via AFM-IR spectroscopy. *Adv. Geo-Energy Res.* **2024**, *13*, 231–236. [CrossRef]
74. Gao, S.; Li, F.; Li, T.; Lu, C.; Lu, Y. Discussion of the relationship between coal metamorphism and the Late Mesozoic basalt in Rujigou Area. *Coal Geol. Explor.* **2003**, *3*, 8–10.
75. Hower, J.C.; Berti, D.; Hochella, M.F.; Rimmer, S.M.; Taulbee, D.N. Submicron-scale mineralogy of lithotypes and the implications for trace element associations: Blue Gem coal, Knox County, Kentucky. *Int. J. Coal Geol.* **2018**, *192*, 73–82. [CrossRef]